

# High Density Polyethylene/Ultra High Molecular Weight Polyethylene Blend. II. Effect of Hydroxyapatite on Processing, Thermal, and Mechanical Properties

K. L. K. Lim,<sup>1</sup> Z. A. Mohd Ishak,<sup>1</sup> U. S. Ishiaku,<sup>2</sup> A. M. Y. Fuad,<sup>3</sup> A. H. Yusof,<sup>4</sup> T. Czigany,<sup>5</sup> B. Pukanzsky,<sup>6</sup> D. S. Ogunniyi<sup>7</sup>

<sup>1</sup>Polymer Engineering Division, School of Materials and Mineral Resources Engineering, Engineering Campus, Universiti Sains Malaysia, 14300 Nibong Tebal, Penang, Malaysia

<sup>2</sup>Department of Advanced Fibro-Science, Kyoto Institute of Technology, Matsugasaki, Sakyo-ku, Kyoto 606-8585, Japan

<sup>3</sup>Plastics and Ceramic Program, SIRIM Bhd, 40911 Shah Alam, Selangor, Malaysia

<sup>4</sup>Department of Orthopedics, School of Medical Sciences, Universiti Sains Malaysia, 15990 Kubang Kerian, Kelantan, Malaysia

<sup>5</sup>Department of Polymer Engineering, Budapest University of Technology and Economics, H-1111, Budapest, Muegyetem rkp.3, Hungary

<sup>6</sup>Department of Plastics and Rubber Technology, Budapest University of Technology and Economics, H-1111, Budapest, Muegyetem rkp.3, Hungary

<sup>7</sup>Department of Chemistry, University of Ilorin, Ilorin 240003, Nigeria

Received 1 March 2005; accepted 30 November 2005

DOI 10.1002/app.22866

Published online in Wiley InterScience (www.interscience.wiley.com).

**ABSTRACT:** Hydroxyapatite (HA) is part of bone mineral composition. Several attempts have been made to incorporate HA into high density polyethylene (HDPE) to produce bone replacement biomaterials since neat HDPE is not suitable as bone replacement. The blending of HDPE with ultra high molecular weight polyethylene (UHMWPE) up to 50% by weight was performed with the aim of improving the toughness of composites. Reinforcement of blend with HA of up to 50% by weight was carried out. Methods of characterizing the composites included density, differential scanning calorimetry, thermal gravimetric analysis, ash content, and morphological

examination using scanning electron microscope. For the mechanical properties of the composites, tensile, flexural, and impact tests were carried out. Incorporation of HA into HDPE has resulted in the brittleness of the composites. Blending of HDPE with UHMWPE in the presence of HA was found to improve the mechanical properties and promote a ductile failure of the resulting composites. © 2006 Wiley Periodicals, Inc. *J Appl Polym Sci* 100: 3931–3942, 2006

**Key words:** biomaterial; high density polyethylene; ultra high molecular weight polyethylene; blend; hydroxyapatite

## INTRODUCTION

Over the years, many approaches have been made to develop bone replacement prostheses, ranging from metal to ceramic to polymeric composites.<sup>1–3</sup> Metals offer high strength but this also causes stress shielding, which result in the loosening of prosthesis.<sup>4</sup> Ceramic was found to have low fracture toughness that lead to brittle failure.<sup>3</sup> Fortunately, polymeric composites seem to be able to offer balance between strength and toughness as properties can be tailored by careful selection of material and processing conditions.<sup>2,5,6</sup> Polymeric composites comprise polymer component

that forms the matrix and the reinforcing phase. Among the polymers used are polyetheretherketone (PEEK), polyaryletherketone (PAEK), polysulfone, epoxy, poly(L-lactic acid) (PLLA), polyhydroxybutyrate, and polyethylene (PE). The reinforcing phase consists of glass fibers, carbon fibers, bioactive glass, and hydroxyapatite (HA).<sup>6–10</sup>

The use of high density polyethylene (HDPE) reinforced with HA has been reported.<sup>7</sup> HA has a structure,  $[Ca_{10}(PO_4)_6OH_2]$ , that is similar to the major inorganic reinforcing phase of bone and its biocompatibility with bone has been reported.<sup>11–13</sup> On the other hand, HDPE is bio-inert and it is analogous to collagen found in bone, providing ductility to the otherwise brittle HA. HDPE filled with HA at high filler loading exhibit brittle properties.<sup>8</sup> Hence, several approaches to further improve the mechanical properties of PE/HA composites were used, including HA selection and treatment (composition, shape, particle sizes, coupling agent) to processing optimization.

Correspondence to: Z. A. Mohd Ishak (zarifin@eng.usm.my).  
Contract grant sponsor: Ministry of Science, Technology, and Environment (MOSTE).

Contract grant sponsor: Universiti Sains Malaysia; contract grant number: IRPA:6010615.

tion.<sup>9,10,14,15</sup> The PE matrix is the component that provides ductility and toughness improvement in this phase and it is expected to improve the overall composite ductility.

Ultra high molecular weight polyethylene (UHMWPE) is another type of PE with extremely high molecular weight ( $4 \times 10^6$ ). It has been widely used as biomaterial, especially as acetabular cup prosthesis in hip replacement surgery.<sup>16,17</sup> UHMWPE offers auto lubrication, which imparts good abrasion resistance, nontoxicity, high impact resistance (even at cryogenic temperature), high toughness, excellent fatigue resistance, and outstanding environmental stress cracking, but unfortunately it has disadvantage in terms of processing.<sup>18–20</sup> This class of PE does not flow even when heated above its melting temperature,  $T_m$ . Because of this nature, filler incorporation is limited to dry mixing. The blend of HDPE with UHMWPE is expected to combine excellent toughness properties of UHMWPE into HDPE while maintaining the processability of HDPE. Our previous work<sup>21</sup> on HDPE/UHMWPE blend showed that HDPE improved the processability of UHMWPE and toughness has been successfully introduced into the blend by the presence of UHMWPE. Up to 50% by weight of UHMWPE addition was found to have optimum properties and good processing.<sup>21</sup> Hence the present work reports on the incorporation of HA into neat HDPE and HDPE/UHMWPE blend and its effects on processability, thermal, morphology, and mechanical properties of the resulting composites.

## EXPERIMENTAL

### Materials and sample preparation

HDPE was supplied by Titan Polyethylene (Malaysia) as Titanex HI 2081 with density of  $0.957 \text{ g/cm}^3$  and melt flow index (MFI) of  $20 \text{ g/10 min}$  at  $190^\circ\text{C}$ . The UHMWPE used was GUR 4120 (Ticona, Germany), supplied in powder form with density of  $0.93 \text{ g/cm}^3$  and no measurable MFI. HA was provided by Merck (catalog no. 102196), with particle sizes ranging from less than 2 to  $20 \mu\text{m}$ . All the composites were prepared by melt mixing in a Brabender Plasticorder Model PLE 331 coupled with a mixer/measuring head (W50H) at  $190^\circ\text{C}$  and a rotor speed of 30 rpm. In the HA-filled HDPE system, HDPE was charged into a Brabender Plasticorder chamber and preheated for 3 min after which mixer rotor was started to crush the HDPE for 1 min. HA was later loaded and mixing stopped at the 20th minute. The mixing of HA-filled HDPE/UHMWPE was similar except that UHMWPE was loaded into the chamber after crushing HDPE for 1 min; blending continued until the 14th minute when HA was loaded and the final mixing stopped at the 20th minute. A two-roll mill was used to sheet out the

TABLE I  
Composition of HDPE/UHMWPE Blend  
and Materials Coding<sup>a</sup>

Label	HA (wt %)	HA (vol %)
HDHA 0	0	0
HDHA 10	10	3.2
HDHA 20	20	6.8
HDHA 30	30	11.2
HDHA 40	40	16.4
HDHA 50	50	22.8
HDUHHA 0	0	0
HDUHHA 10	10	3.2
HDUHHA 20	20	6.8
HDUHHA 30	30	11.2
HDUHHA 40	40	16.4
HDUHHA 50	50	22.8

<sup>a</sup> Ratio of HDPE/UHMWPE blend is at 50 : 50 for HDUH, i.e., HDUHHA 10 refer to HDPE/UHMWPE is at 50 : 50 ratio and 10% weight content of HA.

compound. Thereafter, the mixed compounds were compression-molded into samples using a Gao Tech Hot Press at  $190^\circ\text{C}$ , 14 MPa pressure, for 25 min (including 10 min of preheat). UHMWPE to HDPE ratio of 50 : 50 by weight was used for HA content of 10–50% by weight. Table I shows the label for different composite compositions.

### Characterization

#### Determination of HA particle size and HA content

HA particle size was measured using Malvern Mastersizer. The amount of HA in the composite was measured by ashing at  $650^\circ\text{C}$  for 30 min using Lenton Furnace. Afterwards, the ash obtained was left in a desiccator to cool over silica gel. All weight measurements were carried out at room temperature, using a Mettler AJ 150 weighing balance.

#### Density

The density of test specimens was determined using a pycnometer according to the ASTM D792 water-displacement method (Method A) using the equation

$$\rho = W_1 / (W_1 - W_2) \quad (1)$$

where  $W_1$  and  $W_2$  are sample weights in air and water, respectively. Densities of HDPE, UHMWPE, and HA were quoted by manufacturers as  $0.957$ ,  $0.93$ , and  $3.20 \text{ g/cm}^3$ , respectively. Density based on rule of additivity was calculated as

$$\rho^\circ = \Phi_m \rho_m + \Phi_f \rho_f \quad (2)$$

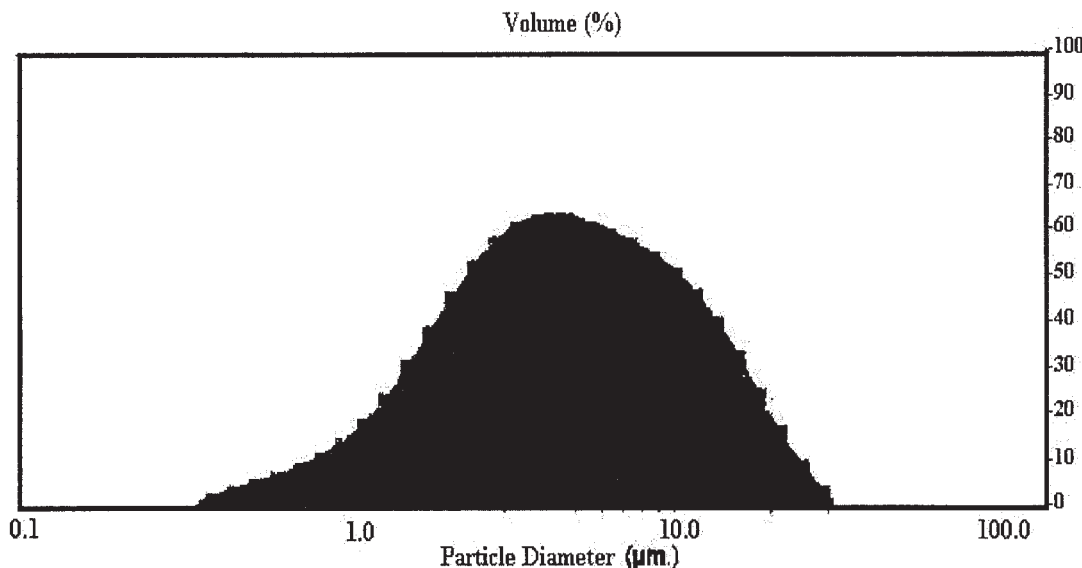


Figure 1 HA particle size distribution.

where  $\rho^\circ$  is the density based on additivity rule,  $\Phi_m$  and  $\Phi_f$  are the volume fraction of matrix and filler;  $\rho_m$  and  $\rho_f$  are the density of matrix and filler, respectively.

#### Differential scanning calorimetry

Thermal analyses were performed on composites using a PerkinElmer DSC 7. Samples of about 5–10 mg were heated to 200°C at a rate of 10°C/min in inert atmosphere and held at 200°C for 1 min before cooling to 30°C at 10°C/min. The same steps were repeated for the second scan. Melting temperature ( $T_m$ ) was the peak in the thermogram and enthalpy ( $\Delta H$ ) was the area under the thermogram. The enthalpy of 100% crystalline polyethylene was assumed to be 293 J/g.<sup>22</sup> Degree of crystallinity ( $\chi$ ) is calculated as

$$\chi = \frac{\Delta H_f}{\Delta H_f^\circ} \times 100 \quad (3)$$

where  $\Delta H_f$  and  $\Delta H_f^\circ$  represent the enthalpy of samples and enthalpy of 100% crystalline PE, respectively.

#### Scanning electron microscopy

The morphology of composite fracture surface was studied with scanning electron microscopy (SEM), using a Leica Cambridge S-360 microscope. All the surfaces were gold-coated to enhance image resolution and to avoid electrostatic charging.

#### Mechanical testing

Dumbbell-shaped tensile test specimen was obtained from compression mold plate with dimension as spec-

ified in ASTM D638 Type I. Tensile test was carried out in accordance with ASTM D638 at test speeds of 5.0 mm/min using a Testometric Model M500.

Flexural test was conducted according to ASTM D790. The test was carried out using a Testometric Model M500 at a test speed of 5.00 mm/min. Span length was fixed at 50.0 mm. The dimension of specimen was 12.7 mm × 3.0 mm × 150.0 mm (width × thickness × length).

Impact test was conducted as specified in ASTM D256 (Izod), using Zwick model 5101 impact tester.

All these tests were conducted at ambient temperature and an average value of five tests was taken for each composition.

## RESULTS AND DISCUSSION

#### Characterization

##### HA particle size

The filler particle size often affects the mechanical properties of composites.<sup>23–27</sup> Hence the characterization of filler size and their distribution will help to understand the properties of composites. Figure 1 shows the particle size distribution of HA powder used in this study. Table II reveals that the median particle size of HA powders used was 4.61 μm. Approximately 10% of the filler is less than 1.40 μm while submicron size is found to be less than 6%. Large particles (20 μm and above) are less than 5%. Overall, filler sizes are fairly distributed and this contributed towards good dispersion of particles up to 40% by weight or 16.4% by volume, as high amount of small particulate matter is reported to have the tendency to agglomerate.<sup>23,28</sup> This will further be discussed in determination of HA content and SEM micrograph.

TABLE II  
HA Particle Size Properties<sup>a</sup>

Sample	Particle size ( $\mu\text{m}$ )			Surface area ( $\text{m}^2/\text{g}$ )
	$D_{0.5}$	$D_{0.1}$	$D_{0.99}$	
HA	4.61	1.4	24.54	2.01

<sup>a</sup>  $D_{0.5}$ , median particle size;  $D_{0.1}$  and  $D_{0.99}$ , the size below which 10% and 99% of the particle diameters lie, respectively.

### HA content and density

HA content and its densities at various HA loading are summarized in Table III. Average HA content for HDHA and HDUHHA suggests that the filler lost during compounding is minimal. At the same time, average deviation and standard deviation values are at less than 5 and 2%, respectively, for both composite systems indicate 'macroscopic' distribution of HA. HDHA displays lower value of deviation when compared to HDUHHA at all HA loadings because of the fact that HDPE has lower viscosity. Lower viscosity allows ease of filler mobility and this contributes toward the dispersion of filler in polymer matrix.<sup>29,30</sup> Even so, when observed, HDUHHA 50 displays certain agglomeration visible to the naked eye. Thus, further examination in terms of microscopic HA distribution by SEM micrographs is essential and will be discussed later.

Densities of composites (Table III) obtained from experiment increase with the increase of filler loading. This observation is expected, since HA density is higher than either HDPE or UHMWPE/HDPE blend. Irrespective of filler loading, the density obtained from experiment shows no significant difference to those calculated by rule of additivity, suggesting the efficiency of mixing of Brabender as little filler is lost

during blending. Ishak et al. reported a similar observation using rice husk as filler in polyolefin.<sup>31</sup>

### Thermal properties

Figure 2 illustrates the typical differential scanning calorimetry (DSC) endotherm of HDUHHA composites at various HA loadings and Table IV provides the DSC results. These data imply that HA filler has some influence on the PE lamellar crystallites as indicated by the shift in melting temperature,  $T_m$ , to lower values. It is believed that melting at lower temperature is associated with thinner lamellar in the composites. Other workers<sup>29-34</sup> have reported the dependence of  $T_m$  on lamellar thickness. HA filler has higher specific heat capacity, thus making it to be a better heat conductor. This in turn causes the cooling of composite to be faster and resulted in thin lamellar formation rather than thick crystal growth.<sup>27</sup>

It is likely that a tail towards the lower temperature region of DSC curve is due to the presence of different crystal distribution. In this case, the tail at lower temperature represents a fraction of very thin crystallites. When  $T_m$  shifts to a lower value, it is expected that the degree of crystallinity would also indicate a lower value. This observation is in agreement with the results presented in Table IV. Although a shift of  $T_m$  to lower temperature is related to formation of thinner lamellar, Bartaczak et al.<sup>29</sup>, in their findings with filled HDPE composites, reported that it is compensated by the formation of larger number of thinner crystallites.

### Brabender torque

Figures 3 and 4 demonstrate the torque development of HDHA and HDUHHA during compounding using Brabender Plasticorder. The processing behavior can

TABLE III  
HA Content after Ashing and Density of Composites at Respective HA Loading<sup>a</sup>

Sample	HA content (%)	Average deviation (%)	Standard deviation	Experimental density, $\rho$ ( $\text{g}/\text{cm}^3$ )	Theoretical density, $\rho^0$ ( $\text{g}/\text{cm}^3$ )
HDHA 0				0.97	0.96
HDHA 10	10.20	0.77	0.08	1.05	1.02
HDHA 20	19.39	0.85	0.17	1.14	1.10
HDHA 30	29.53	0.56	0.17	1.23	1.19
HDHA 40	39.06	0.86	0.33	1.35	1.30
HDHA 50	49.08	2.57	1.26	1.45	1.43
HDUHHA 0				0.96	0.94
HDUHHA 10	10.99	4.37	0.48	1.03	1.01
HDUHHA 20	19.60	1.69	0.33	1.11	1.08
HDUHHA 30	29.45	1.65	0.49	1.21	1.17
HDUHHA 40	38.41	4.58	1.76	1.29	1.28
HDUHHA 50	47.84	3.23	1.54	1.41	1.41

<sup>a</sup> Ratio of HDPE/UHMWPE blend is at 50 : 50 for HDUH, i.e., HDUHHA 10 refer to HDPE/UHMWPE is at 50 : 50 ratio and 10% weight content of HA.

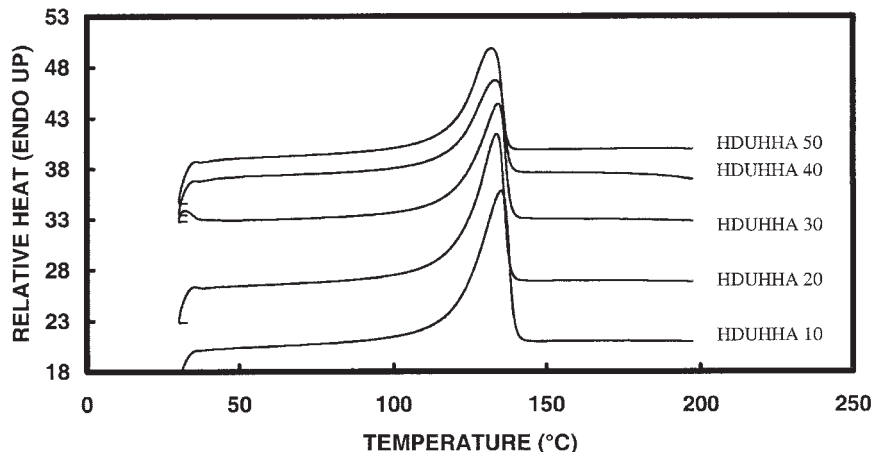


Figure 2 Differential scanning calorimetry of HDUHHA at various HA loadings.

be seen through torque development in Brabender.<sup>35-37</sup> It also provides a window to the viscosity and processability of composites. Initial torque peak in HDHA labeled as A in Figure 3 is due to the melting of HDPE. The second torque peak at B occurs when HA filler is charged into the mixing chamber. The torque increase is anticipated, as HA is more rigid, thus it will restrict the flow of polymer. Moreover, HA filler initially is cooler when compared with the melt in the mixing chamber. Thus, these reasons lead to the second torque peak observed. After  $\sim$ 10 min of mixing, the torque development reaches a plateau at C, indicating no significant change in viscosity. The torque values at B and C recorded higher values as HA loading increases because HA filler has a higher rigidity that poses a hindrance to flow.

Figure 4 depicts the torque development for HDUHHA as filler content increases. The first torque peak labeled A represents the melting of HDPE. The second

torque with a maximum at B reflects the charging of UHMWPE that is cooler initially when compared with the melt in the mixing chamber. The third torque peak has a type of plateau (indicated by C) that is attributed to the fusion of HDPE and UHMWPE components of the blend. HDUHHA system shows decrease in torque when filler loading is increased, as noticed at points D and E in Figure 4 (charging of HA into mixing chamber). This observation is believed to relate to the higher viscosity of blend. Higher viscosity gives rise to reduced flow, resulting in difficulties of filler incorporation. Even so, the effect of filler incorporation is minimal as the result shown earlier in ashing and Thermal gravimetric analysis (TGA) reflects efficient incorporation of filler into both composite systems. It is postulated that HA filler at later stage of mixing forms a noncontinuous layer separating mixing chamber wall from the composite blend, causing lower friction between mixing chamber wall and the

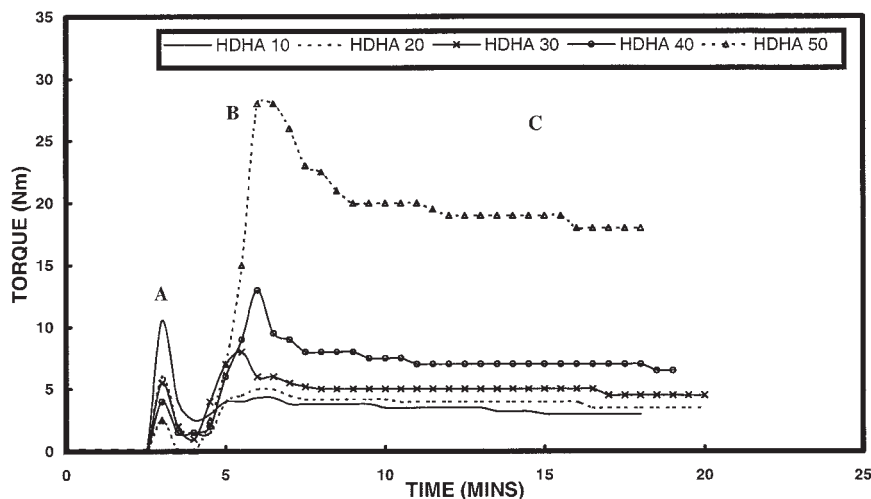


Figure 3 Torque development curve of HDHA in Brabender at various HA loadings.

TABLE IV  
Thermal Properties of HDUHHA Composites at Various HA Content<sup>a</sup>

Sample	Melting temperature, $T_m$ (°C)	Enthalphy, $H_f$ (J/g)	Degree of crystallinity, $\chi$ (%)
HDUHHA 0	135.8	175	59.7
HDUHHA 10	135.3	149	50.8
HDUHHA 20	134.0	127	43.3
HDUHHA 30	134.4	116	39.6
HDUHHA 40	133.5	109	37.2
HDUHHA 50	132.1	116	39.6

<sup>a</sup> Ratio of HDPE/UHMWPE blend is at 50:50 for HDUH, i.e., HDUHHA 10 refer to HDPE/UHMWPE is at 50:50 ratio and 10% weight content of HA.

rotating rotor. This contributes to the lower torque obtained at the end of mixing as HA filler increases. In particular, at high HA loading (HDUHHA 40 and HDUHHA 50), an extra torque peak is noticed at point X. This is possibly due to the migration of HA to the interface between mixing chamber wall, and composite and rotor. Subsequently lower torque was observed. It is possible that HA filler has a little affinity towards metal.

The higher viscosity of the blend brings about lower flow, hence introducing restriction to the flow of matrix and subsequently the dispersion of filler. The results here agree with earlier observation concerning HA content and the standard deviation of HA content.

## Mechanical properties

### Tensile property

Figure 5 presents the Young's modulus of HDHA and HDUHHA composites at various HA loadings. Maximum filler loading of HDHA is 11.2% by volume or 30% by weight because HDHA with higher filler content is too brittle to be compression-molded. On the contrary, HDUHHA composites are capable of loading up to 22.8% by volume or 50% by weight. This observation is not anticipated, as earlier result in ashing, TGA, and torque development studies indicate easier HA incorporation into the HDPE matrix. Hence it is proposed that the ease of incorporation of HA into the matrix does not necessarily dictate higher strength of composites. HDPE has lower viscosity and this enables the ease of filler incorporation, while HDPE/UHMWPE blend has higher viscosity that suggests better melt strength. Thus, it can be molded into specific shape and retain the dimension upon cooling, as opposed to HDPE. Since the HDPE component of both composites is the same, it is apparent that the 'extra' strength is contributed by UHMWPE component itself. Bonfield et al.<sup>7</sup> reported the loading of HA up to 45% by volume into HDPE. This could be attributed to the following reasons: the use of twin screw extruder that introduces high shear and further powdering of pellet in centrifugal mill using liquid nitrogen. In addition, molding of composites is in plate form at 205°C before being machined to dumbbell shape using a

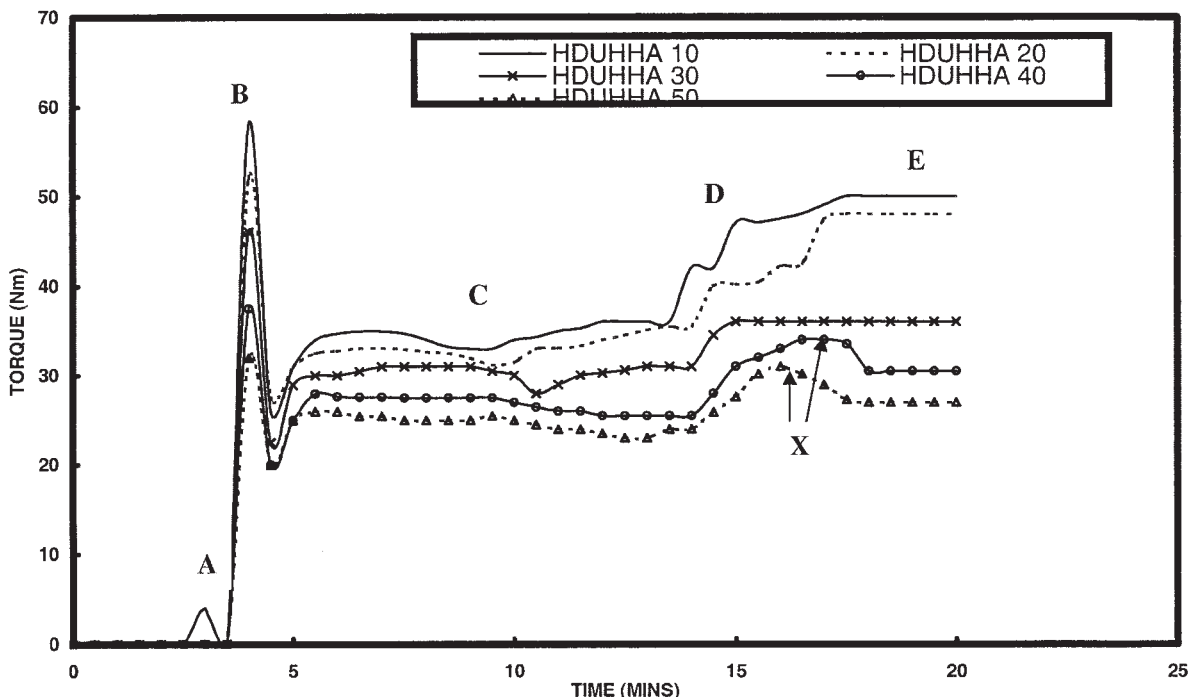


Figure 4 Torque development curve of HDUHHA in Brabender at various HA loadings.

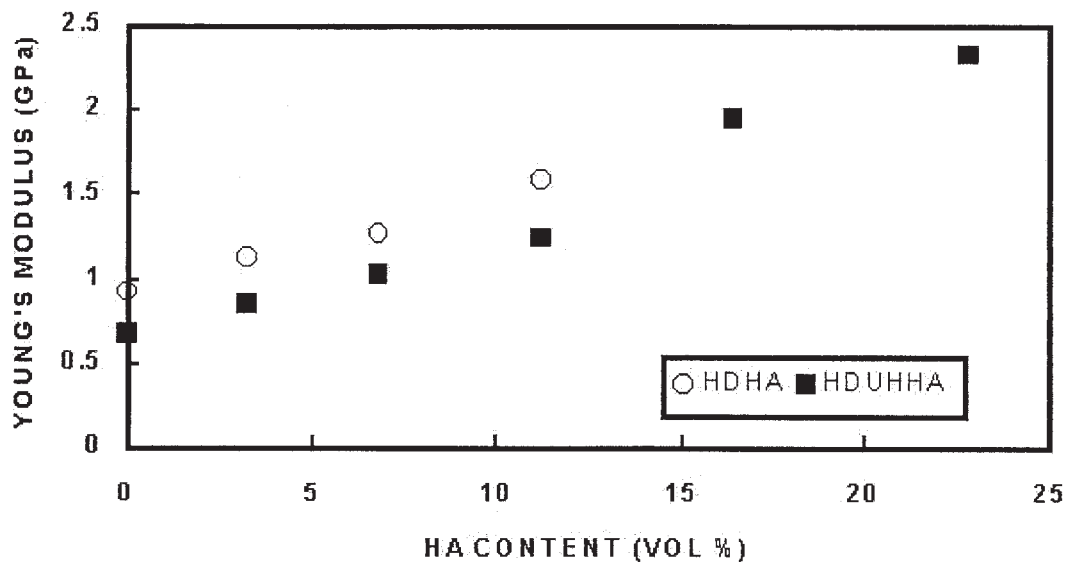


Figure 5 Young's modulus of HDHA and HDUHHA at various HA loadings.

pantograph machine. The system here uses much simpler processing route to reduce the cost of production and other complications that may arise from multiple processing. Thus by applying the processing route suggested by Wang et al.,<sup>10</sup> it is expected that the higher loading of HA into HDPE composite system is possible. This is proven in flexural sample capable of sustaining HA loading up to 22.8% by volume by molding into plate first before being cut into the appropriate dimension for flexural test.

The comparison of Young's modulus of both composites reveals that HDHA has higher Young's modulus than HDUHHA with the same amount of filler loading (Fig. 5). However, because of the ability of HDUHHA composites to sustain higher HA loading, the final Young's modulus was higher than that of

HDHA. It is believed that the blend has allowed the extension of filler loading by increasing the overall melt strength and toughness. Increment of modulus due to filler with higher rigidity than the matrix has been reported by other workers.<sup>27,38,39</sup>

Figure 6 shows the effect of filler loading on the tensile strength of composites. HDUHHA composites are observed to show reasonably higher tensile strength when compared with HDHA system. The interaction between filler and matrix is poor because one component is inorganic (HA) while the other is organic (PE). Because of this fact, the addition of filler into the matrix may introduce weak points that subsequently manifest as stress concentration in the composite.<sup>40</sup> When stress is applied, because of poor filler-matrix interaction when compared with matrix-ma-

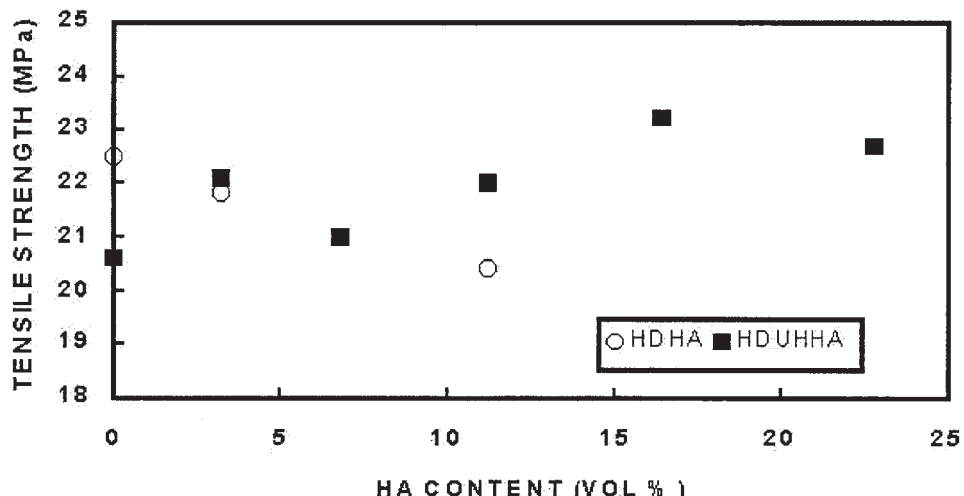


Figure 6 Tensile strength of HDHA and HDUHHA at various HA loadings.

TABLE V  
Tensile Strain and Energy at Break for HDHA and HDUHHA Composites at Different HA Loading<sup>a</sup>

HA loading (wt %)	(vol %)	HDHA		HDUHHA	
		Tensile Strain (%)	Energy at Break (Nm)	Tensile Strain (%)	Energy at Break (Nm)
0	0	241	68.2	20.6	427.5
10	3.2	7.5	5.3	22.1	328
20	6.8	3.9	2.4	21	20.7
30	11.2	2	1	22	16.2
40	16.4			23.2	3.1
50	22.8			22.7	1

<sup>a</sup> Ratio of HDPE/UHMWPE blend is at 50 : 50 for HDUH, i.e., HDUHHA 10 refer to HDPE/UHMWPE is at 50 : 50 ratio and 10% weight content of HA.

trix interaction, separation of filler from matrix is quite likely to initiate at filler–matrix interface, leading to development of void, debonding of fillers and subsequently crack and failure of composites. This explains the poor tensile strength of HDHA at higher HA loading. In addition, at high filler content, apart from filler–matrix interaction, filler–filler interaction also plays a role in the decrease of tensile strength. Bonfield et al.<sup>7</sup> as well as Suwanprateeb<sup>41</sup> pointed out similar observation in HDPE-filled HA system and HDPE-filled calcium carbonate system, respectively.

In the case of HDUHHA, the composite is able to maintain a fairly constant tensile strength or at least a slight improvement with filler loading up to 22.8% by volume (50% by weight). This observation is attributed to the possibility of UHMWPE's extremely long chains trapping HA particles in the matrix, leading to enhanced mechanical interlock. The values of tensile strain and energy at break are summarized in Table V and a comparison of the values for HDHA and for HDUHHA shows the latter to be far more superior. It also shows that the formation of fibrils is also related

to plastic deformation, which helps to increase ductility of composites. As the loading of HA in the composite increases, there is a reduction of tensile strain and energy at break for both HDHA and HDUHHA systems, but HDUHHA still demonstrates remarkable superiority over HDHA composites. A possible reason for this phenomenon may be due to crack that initiates from the interface of HA particle in HDHA and acts as points of stress concentration. Because of relatively high crack resistance of UHMWPE, formation of void,<sup>42</sup> and the crack propagation is slowed down as UHMWPE absorb part of the energy. This mechanism is proposed to explain why blend composites (HDUHHA) have considerable better toughness when compared with HDPE.

#### Flexural property

Figure 7 shows the flexural modulus of composites at various filler compositions. Unlike tensile sample, which is molded out from tensile-shaped cavity, samples for flexural investigation were molded out in

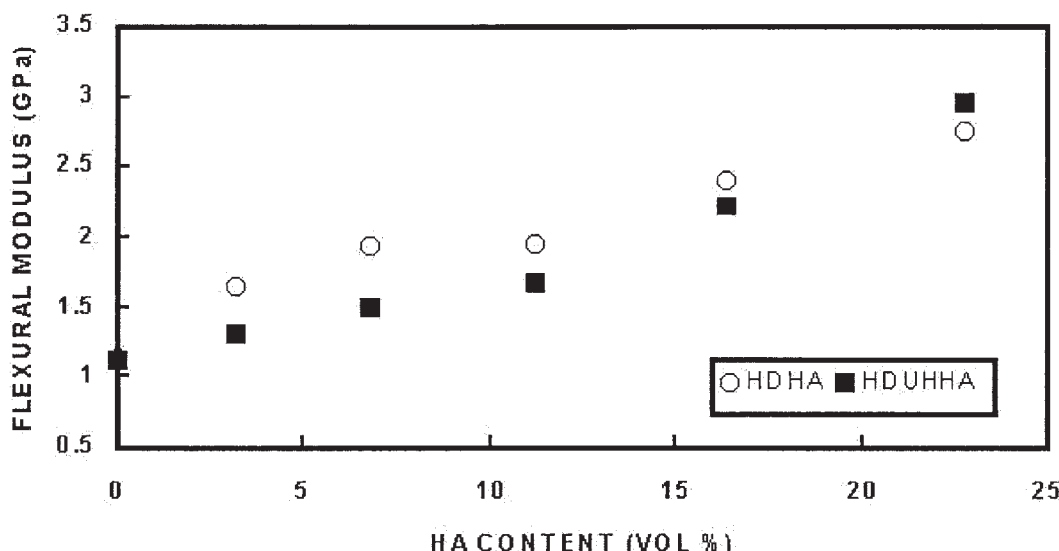


Figure 7 Flexural modulus of HDHA and HDUHHA at various HA loadings.

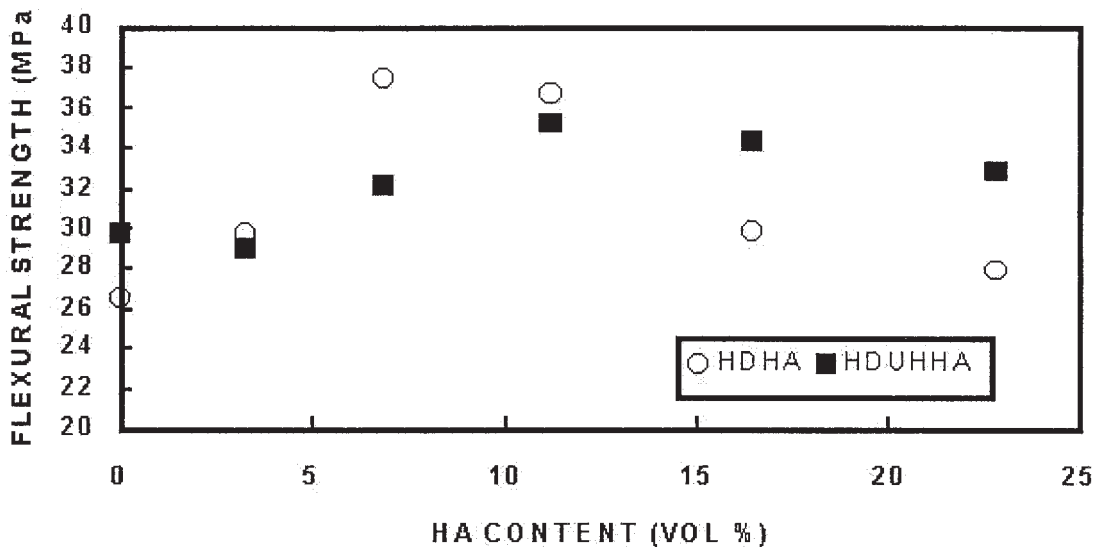


Figure 8 Flexural strength of HDHA and HDUHHA at various HA loadings.

plate form and cut with rotating band saw for the required flexural test dimension. Thus, up to 22.8% by volume or 50% by weight of HA in both HDHA and HDUHHA composites could be produced. Flexural modulus of HDHA was consistently higher than HDUHHA but at 50 wt % HA, HDUHHA had higher flexural modulus than the corresponding HDHA samples.

The lower flexural strength of HDHA compared with HDUHHA at higher HA content is shown in Figure 8; it indicates that the higher rigidity of HDHA leads to brittle characteristic, in which failure occurs before the sample is able to reach its real strength. Brittle failure occurs when applied stress is unable to

be fairly distributed, causing local stress concentration that leads to crack formation especially near defects, frozen stress area, particle-matrix interface, and particle-particle interface. Because of the inefficiency of stress distribution, debonding of particle initiated at these weak points leads to further interruption of stress distribution. When the separation grows large enough, crack propagation occurs. Eventually, more stress is concentrated on the neighboring particles from the advancing crack, bringing about rapid and successive propagation that finally leads to brittle failure. From Figure 8 it can be seen that the flexural strength of HDHA start to decrease from HA content of 6.8% by volume (20% by weight). In contrast, HDU-

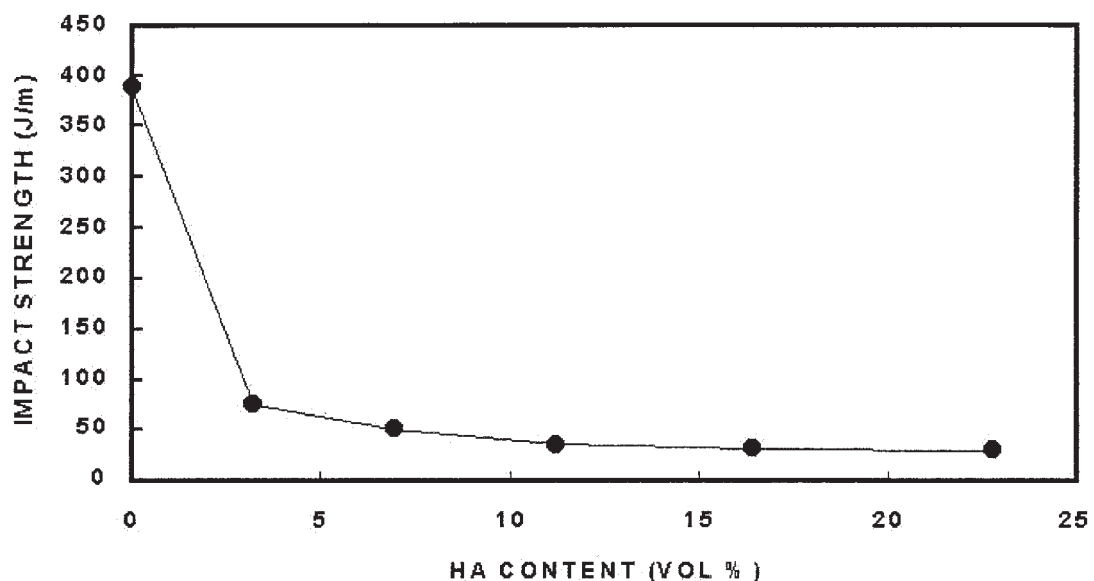
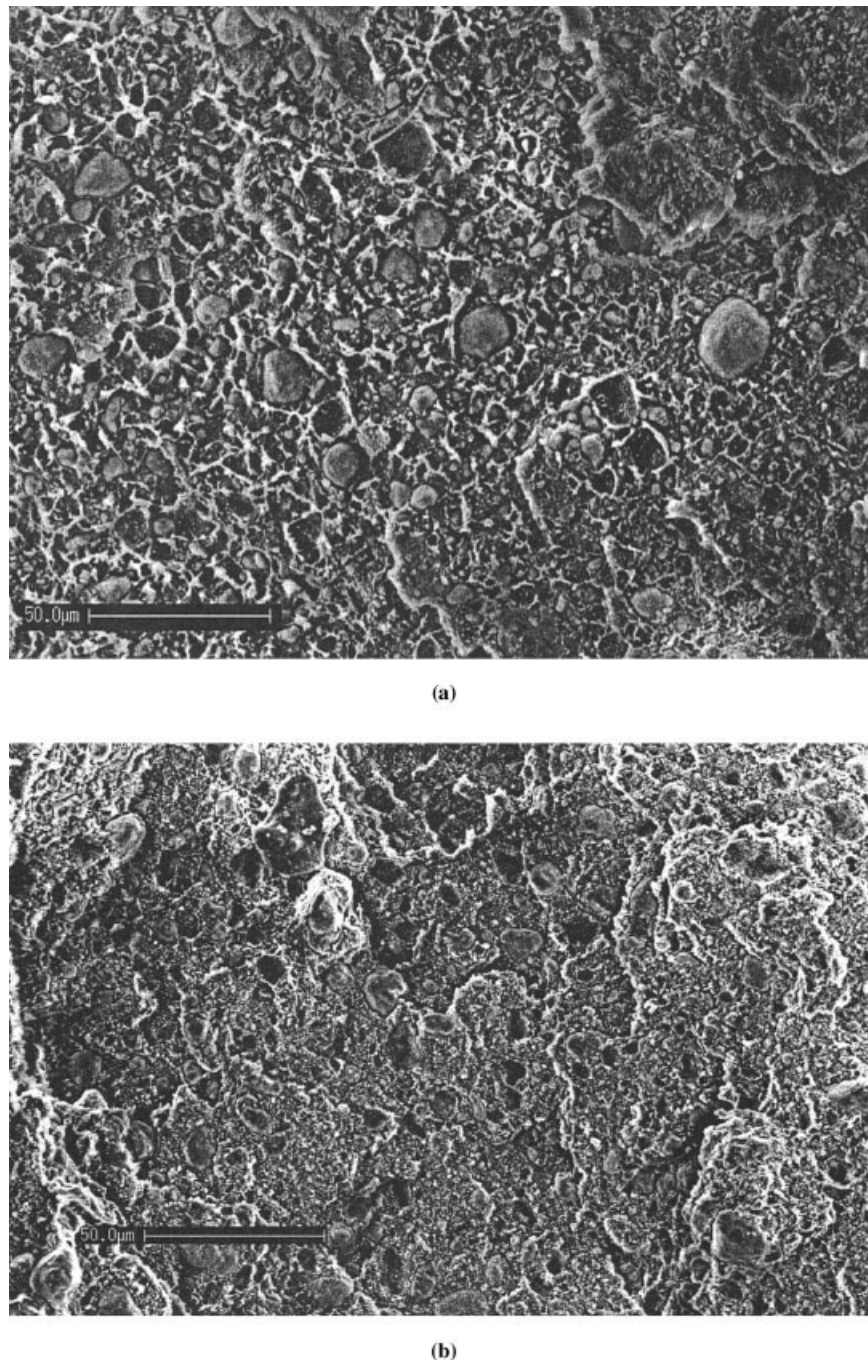


Figure 9 Impact strength of HDUHHA at various HA loadings.



**Figure 10** (a) SEM micrograph of HDHA 20 tensile fracture surface at 500 $\times$  magnification.(b) SEM micrograph of HDHA 40 tensile fracture surface at 500 $\times$  magnification.

HHA composites show a rather stable flexural strength at high filler loading.

#### Impact property

The impact strength data, presented in Figure 9, shows a reduction in impact strength after the addition of HA filler to HDPE/UHMWPE blend. Impact strength shows obvious decrease in value after the

initial loading of HA filler. This is anticipated because, the introduction of filler into polymer matrix<sup>43</sup> disrupts the continuity of the matrix and may be explained as follows. Before the inclusion of HA filler, UHMWPE interaction with HDPE is strong since both have the same chemical composition. Because of this, it gives rise to high impact strength for the unfilled blend. When HA is introduced, the HDPE/UHMWPE area of contact decreases and is replaced by HA/

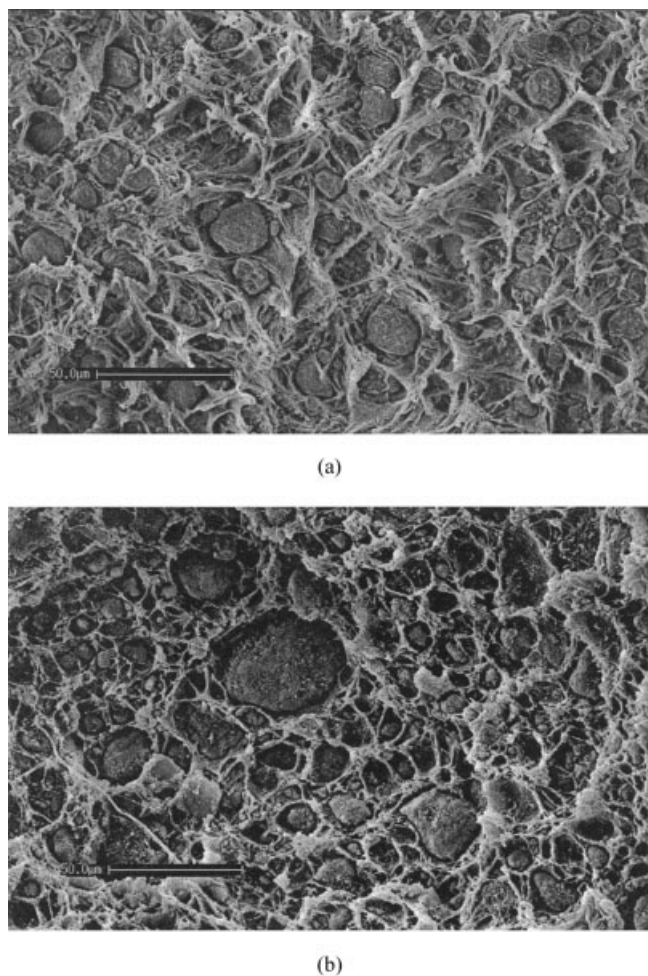


**Figure 11** (a) SEM micrograph of HDUHHA 20 tensile fracture surface at 500 $\times$  magnification. (b) SEM micrograph of HDUHHA 40 tensile fracture surface at 500 $\times$  magnification.

HDPE and HA/UHMWPE contact area. HA has relatively low compatibility with PE. This in turn lowered the capability of matrix to distribute the impact energy applied. However, it is worth noting that after the initial sharp decrease, impact strength seems to remain stable regardless of subsequent increase in HA loading. Toughness enhancement by UHMWPE phase also reveals itself in the morphological failure surface observed in SEM micrograph, which will be discussed subsequently.

#### Scanning electron microscopy

Figures 10 and 11 show the fracture surface of HDHA and HDUHHA at different filler loadings. At 6.8% by volume of filler loading in HDHA, some plastic deformation can be spotted [Fig. 10(a)] but at higher filler loading, brittle fracture is observed as indicated by the random flake-like rough surface [Fig. 10(b)]. This structure is often associated with brittle failure.<sup>44</sup> The

effect of higher filler loading in reducing matrix deformation has been reported elsewhere.<sup>39</sup> In comparison to HDHA composites, HDUHHA system provide reasonable proof of better plastic deformation at the corresponding filler loadings, as shown in Figure 11. Figure 11(a) shows extensive fibril formations of HDUHHA 20 compared with HDHA 20 in Figure 10(a) at the same magnification. The same trend is also observed for higher filler percentage in Figures 10(b) and 11(b), respectively. For HDUHHA system, increase of filler leads to decrease in the formation of fibrils, indicating lower ductility of material. Wang et al. made a similar observation for the failure behavior of HA/HDPE.<sup>10</sup>

Generally, HA exhibits poor bonding towards PE in both composite systems, as depicted in particle debonding and existence of voids between particles and matrix. The clean HA surface without obvious PE fibrils sticking on the surface implies the weak bonding of HA to PE. It is concluded that HA particles are mechanically locked by PE matrix of both composites. It is apparent that HDUHHA system provides better mechanical interlock by the more enclosed HA particle in Figure 11(a) when compared with HDHA in Figure 10(a). It is postulated that UHMWPE, which has high molecular weight chains, is capable of extensive fibrils formation, which contribute to the enhanced mechanical interlock of HA particles. It may be possible that further treatment of HA particle with coupling agent would help to introduce chemical interaction of HA and PE matrix. This will be the subject of our future publication.

#### CONCLUSIONS

The following conclusions can be drawn from this study

1. Density values of HA-reinforced HDPE and HA-reinforced HDPE/UHMWPE indicated little filler loss during compounding of the samples. Ashing and TGA further support this observation. TGA also show that there is increase in thermal stability of the filled composites with increased HA content.
2. HA introduces rigidity into the composites, as shown in Brabender torque studies. This rigidity in turn brings about brittle characteristic into the composite properties, as observed in the mechanical properties. However, composites containing UHMWPE are found to have better toughness than those without. Thus it is concluded that the incorporation of UHMWPE into HDPE has successfully introduced toughening effect into HDPE. Also, this toughening effect is, to some extent, sustainable in HA reinforced HDPE/UHMWPE composite system.

3. Toughness improvement of HDPE/HA system by the presence of UHMWPE is further supported by failure mechanism observed using SEM. Extensive plastic deformation in the form of fibril formation is believed to be the main toughening mechanism.

This work was part of a Malaysian–Hungarian Intergovernmental Scientific and Technology Program. Dr. D.S. Ogunniyi is the recipient of USM Postdoctoral Fellowship in Research. Also, D.S.O. is grateful to the administration of University of Ilorin, Nigeria, for the award of a study leave.

## References

1. Evans, S. L.; Gregson, P. J. *Biomaterials* 1998, 19, 1329.
2. Johnnna, S. T.; Antionios, G. M. *Biomaterials* 2000, 21, 2405.
3. Marc, L.; Rack, H. J. *Biomaterials* 1998, 19, 1621.
4. Margaret, A. M.; Donald, W. H.; Kerry, C.; David, R. H.; Corinna, I. W.; Mark, J. P.; Jean, D. M. *Wear* 2000, 241, 158.
5. Nela, A.; David, H. *TIBTECH* 1999, 17, 409.
6. Ramakrishna, S.; Mayer, J.; Wintermantel, E.; Kam, W. L. *Compos Sci Technol* 2001, 61, 1189.
7. Bonfield, W.; Grynpas, M. D.; Tully, A. E.; Bowman, J.; Abram, J. *Biomaterials* 1981, 2, 185.
8. Wang, M.; Porter, D.; Bonfield, W. *Br Ceram Trans* 1994, 93, 91.
9. Wang, M.; Berry, C.; Braden, M.; Bonfield, W. *J Mater Sci: Mater Med* 1998, 9, 621.
10. Wang, M.; Joseph, R.; Bonfield, W. *Biomaterials* 1998, 19, 2357.
11. Chang, B. S.; Lee, C. K.; Hong, K. S.; Youn, H. J.; Ryu, H. S.; Chung, S. S.; Park, K. W. *Biomaterials* 2000, 21, 1291.
12. Yuan, H.; Kenji, K.; de Brujin, J.; Li, Y.; Groot, K.; Zhang, X. A. *Biomaterials* 1999, 20, 1799.
13. Ugo, R. *Biomaterials* 1996, 17, 31.
14. Wang, M.; Ladizesky, N. H.; Tanner, K. E.; Ward, I. M.; Bonfield, W. *J Mater Sci* 2000, 35, 1023.
15. Suwanprateeb, J.; Tanner, K. E.; Turner, S.; Bonfield, W. *J Biomed Mater Res* 1998, 39, 16.
16. Baker, D. A.; Hasting, R. S.; Pruitt, L. *Polymer* 2000, 41, 795.
17. Bellare, A.; Cohen, R. E. *Biomaterials* 1996, 17, 2325.
18. Cook, J. T. E.; Klein, P. G.; Ward, I. M.; Brain, A. A.; Farrer, D. F.; Rose, J. *Polymer* 2000, 41, 8615.
19. Kang, P. H.; Nho, Y. C. *Radiat Phys Chem* 2001, 60, 79.
20. Boscolo, B. A.; Franco, R.; Scapin, M.; Tavan, M. *Eur Polym J* 1995, 33, 97.
21. Lai, K. L. K.; Ishak, Z. A. M.; Ishiaku, U. S.; Fuad, A. M. Y.; Yusof, A. H.; Czigany, T.; Pukansky, B.; Ogunniyi, D. S. *J Appl Polym Sci* 2005, 97, 413.
22. Pasto, A. E.; Braski, D. N.; Watkins, T. R.; Porter, W. D.; Lara, C. E.; McSpadden, S. B. *Compos B* 1999, 30, 631.
23. Karger-Kocsis, J. *Polypropylene: Structure, Blends and Composites*; Chapman and Hall: London, 1995; p 1.
24. Schlumpf, H. P. In the 10th International Macromolecule Symposium; Switzerland, September 1990.
25. Schlumpf, H. P. *Kunststoffe* 1983, 73, 511.
26. Samuel, R. J. *Structured Polymer Properties*; Wiley: New York, 1974.
27. John, M. *Additives for Plastics Handbook*; Elsevier: Oxford, 1996; p 23.
28. Geoffrey, P. *Plastics Additives: An A–Z Reference*; Chapman and Hall: London, 1998; p 241.
29. Bartaczak, Z.; Argan, A. S.; Cohen, R. E.; Winberg, M. *Polymer* 1999, 40, 2347.
30. Silva, A. L. N.; Rocha, M. C. G.; Moraes, M. A. R.; Valente, C. A. R.; Coutinho, F. M. B. *Polym Test* 2002, 21, 57.
31. Ishak, Z. A. M.; Yow, B. N.; Ng, B. L.; Khalil, H. P. S. A.; Rozman, H. D. *J Appl Polym Sci* 2001, 81, 742.
32. Paul, W. B. *Hydroxyapatite and Related Material*; CRC Press: London, 1994; p 45.
33. Tang, L. P.; Ng, C. H.; Wang, M. *Manufacture and Thermo-physical Properties of Hydroxyapatite Reinforced High Density Polyethylene*; Technical Report, School of Mechanical and Production Engineering, NTU, Singapore, 1998; p 502.
34. Wunderlich, B. *Macromolecular Physics*, Vol. 2; Academic Press: New York, 1976; p 88.
35. Mathew, W. Y.; George, E.; Francis, D. J. *Int J Polym Mater* 1993, 21, 189.
36. Ishiaku, U. S.; Ismail, H.; Ishak, Z. A. M. *J Appl Polym Sci* 1998, 73, 75.
37. Mousa, A.; Ishiaku, U. S.; Ishak, Z. A. M. *Plast Rubber Compos Process Appl* 1997, 26, 331.
38. Reis, R. L.; Cunha, A. M.; Oliveira, M. J.; Campos, A. R.; Bevis, M. J. *Mater Res Innovat* 2001, 4, 263.
39. Sim, C. P.; Cheang, P.; Liang, M. H.; Khor, K. A. *J Mater Process Technol* 1997, 22, 75.
40. Wang, M.; Bonfield, W. *Biomaterials* 2001, 22, 1311.
41. Suwanprateeb, J. *J Appl Polym Sci* 1999, 75, 1503.
42. Aiba, M.; Osawa, Z. *Polym Degrad Stabil* 1998, 61, 1.
43. Zhang, Y.; Tanner, K. E. *J Mater Sci: Mater Med* 2003, 14, 63.
44. Jenkin, A. D. *Polymer Science*, Vol. 1; North Holland: Amsterdam, 1972; p 630.